Liquid crystal biosensor with aptamer recognition for highly sensitive and quantitative norfloxacin detection via whispering gallery mode

Peiyao An, Mengxiao Li, Shanshan Zhang, Zhenqi Cao, Miao Yu, Tangcheng Huang, Duo Wang, Yue Li, Rensheng Shen, Xin Yang, Jun Ren, Zhenlin Wu

PII: S0026-265X(25)04118-9

DOI: https://doi.org/10.1016/j.microc.2025.116766

Reference: MICROC 116766

To appear in: *Microchemical Journal*

Received date: 27 November 2025

Revised date: 26 December 2025

Accepted date: 30 December 2025

Please cite this article as: P. An, M. Li, S. Zhang, et al., Liquid crystal biosensor with aptamer recognition for highly sensitive and quantitative norfloxacin detection via whispering gallery mode, *Microchemical Journal* (2024), https://doi.org/10.1016/j.microc.2025.116766

Liquid Crystal biosensor with aptamer recognition for highly sensitive and quantitative Norfloxacin Detection via Whispering Gallery Mode

Peiyao An,[a] Mengxiao Li,[a] Shanshan Zhang,[a] Zhenqi Cao,[a] Miao Yu,[a] Tangcheng Huang,[a] Duo Wang,[a] Yue Li,[b] Rensheng Shen,[c] Xin Yang,[d] Jun Ren[e] and Zhenlin Wu*[a]

[a.] School of Optoelectronic Engineering and Instrumentation Science, Dalian University of Technology, Dalian, 116024, China.

[b.] Dalian Women and Children's Medical Group, Dalian, 116033, China.

[c.] School of Integrated Circuits, Dalian University of Technology, Dalian, 116024, China.

[d.] Department of Electrical and Electronic Engineering, School of Engineering, Cardiff University, Cardiff CF24 3AA, United Kingdom.

[e.] School of Bioengineering, Dalian University of Technology, Dalian, 116024, China.

*. Corresponding author. E-mail: zhenlinwu@dlut.edu.cn.

Abstract

As the fluoroquinolone antibiotics, norfloxacin has the advantages of antibacterial properties and efficient inhibition of bacterial DNA replication. Because of its strong binding affinity toward DNA helicases, this compound is chemically stable and exhibits limited biodegradation in environmental matrices. Prolonged use or discharge can enrich antibiotic resistance genes among microbial communities and contribute to persistent contamination. Herein, a nematic liquid crystal (LC) microlaser based on an aptamer recognition was reported and explored its application of norfloxacin ultrasensitive detection in soil. The rapid, real-time and quantitative monitoring of norfloxacin was achieved by exploiting whispering gallery mode (WGM) resonances in LC microdroplets functionalized with a specific aptamer as the molecular recognition element. Through resonance simulation and size-dependent experiments, the feasibility of using LC microlaser as a WGM microresonator was demonstrated. The optimal concentration of CTAB and DNA aptamer was 1 μM and 100 nM, respectively, which could realize the configuration transition of LC microdroplets from radial to bipolar. The devised norfloxacin sensor showed high sensitivity with a detection limit of 0.3 ng/mL, which was an order of magnitude lower than that reported for polarized optical microscope (POM) methods. In addition, the successful detection of various concentrations of norfloxacin in soil samples underscored the practical utility in environmental monitoring. The aptamer-based WGM-LC microlaser provides a highly sensitive approach for norfloxacin detection. The laser recognition probe does not require fluorescent or chromogenic labels, which affords significant advantages for rapid, real-time, and quantitative biosensing. This platform is expected to be extensible to ultrasensitive detection of other drugs, proteins, or environmental pollutants,

particularly suited for integration into microfluidic devices for on-site environmental monitoring and public health risk assessment.

Keywords: liquid crystal (LC) biosensor; whispering gallery mode (WGM); label free; DNA aptamer; norfloxacin (NOX)

1. Introduction

The identification and development of antibiotics have profoundly transformed the structure and function of the health care system. Their sustained application has substantially contributed to the prevention and control of infectious diseases over multiple decades[1]. Norfloxacin (NOX) was the first discovered fluoroquinolone antibiotic[2]. As a broad-spectrum antibacterial drug, Norfloxacin (NOX) has been widely used in medical and veterinary fields because of its high efficiency in inhibiting bacterial DNA replication[3,4]. However, excessive intake of norfloxacin can cause a series of adverse reactions, such as gastrointestinal discomfort, liver and kidney damage, and antibiotic resistance. Some countries have established maximum residue levels for norfloxacin in different animal-based foods to effectively monitor the antibiotics levels in different food matrices[5,6]. However, most antibiotics are non-biodegradable, their presence even at very low concentrations (ng/L) could lead to antimicrobial resistance, which is a serious environmental problem. Therefore, testing whether norfloxacin residues comply with safety standards is essential for ensuring environmental safety and the health of consumers. At present, a range of analytical approaches, including the electrochemical method, fluorescent spectroscopy[7,8] enzyme-linked immunosorbent assay (ELISA) [9], high performance liquid chromatography (HPLC)[10,11] were widely employed for the detection of norfloxacin in milk and aquatic samples.

Liquid crystals (LCs), as a unique functional material, have been gradually used to develop chemical and biological sensors due to their excellent performance in biocompatibility, high sensitivity response and flexibility[12,13]. LCs are utilized as signal amplifiers to detect and report minute molecular events and external perturbations at LC/aqueous interfaces. Researchers usually identify anchoring changes in LC molecules with polarization light microscopy (POM). POM observation techniques have been successfully used to detect surfactants, lipids[14], vapors[15], proteins[16–18], and synthetic polymers[19]. However, the POM detection method relies on subjective visual observation, making it difficult to achieve quantitative and high-precision detection. This limitation becomes a major constraint in most applications of LC-based sensors. Recent researches have shown that spectral detection of target molecules is a more sensitive method. For example, *Liu et al.* proposed a LC-amplified optofluidic sensor for bovine serumalbumin detection, achieving a detection limit of 1 fM[20]. *Yang et al.* introduced a microbubble-based optical barcodes designed to achieve both highly precision and wide-range temperature detection[21].

However, Microbubble configurations are subject to alterations due to surrounding environmental factors. As an illustration, producing microbubble cavities is complicated and the consistency is difficult to guarantee. The microbubble cavity structure has high sensitivity to environmental interference. The microbubble cavities are typically coupled to optical fiber tapers to achieve

whispering gallery mode. However, this coupling method is susceptible to distance and alignment errors, which can limit coupling efficiency. LC droplets doped with dyes can support the WGM laser and act as a sensing probe itself. This new detection method provides an effective way to overcome the limitations of traditional POM methods.

Nucleic acid aptamers are short, single-stranded oligonucleotides (DNA or RNA) that are obtained through the systematic evolution of ligands by exponential enrichment (SELEX) technology [22]. The aptamers can specifically bind various target molecules, including proteins, cells, small molecules, and bacteria, with high sensitivity and strong affinity [23]. In the aptasensors, the detection mechanism follows a conformational change triggered by the binding of the target molecule, like the development of a G-quadruplex upon target binding [24,25]. These properties render aptamers highly attractive as molecular recognition probes in a wide range of biosensor applications. In recent years, applications of aptamer-based LC biosensors have been rapidly developed owing to the excellent target recognition and binding capabilities of aptamers, which significantly enhance the selectivity of the sensors [26–28]. The integration of LC materials with aptamer has emerged as a key approach to developing highly specific biosensing platforms.

In this work, an innovative liquid crystal-based sensing platform is constructed for norfloxacin (NOX) detection, utilizing a DNA aptamer as the molecular recognition element. The LC microdroplets are used as sensing elements and sample pools for the analysis of trace samples. Surfactants CTAB can control the orientation of liquid crystals in droplets by affecting interfacial orientation. When norfloxacin binds to its specific DNA aptamers, this interaction disrupts the vertical alignment of the liquid crystal molecules, ultimately enabling qualitative detection of 5CB microlaser from bipolar to radial configuration. The practicality of employing LC microdroplets as the optical microresonator has been demonstrated by the combination of simulation and experiments. Through the synergistic amplification effect provided by both WGM resonance and 5CB molecules, the biological reaction response observed at the interface could be greatly increased. The detection limit of 0.3 ng/mL norfloxacin could be achieved. The quantification, effectiveness and sensitivity of the WGM spectral analysis method are verified by comparison with POM methods. At the same time, the sensor has also been verified in the soil sample.

2 Working Mechanism

When light propagated along the equatorial region near the surface of the WGM microlasers, total internal reflection occurred inside the microresonator because of refractive index (RI) difference between the microcavity and the surrounding medium. This phenomenon enabled the light to repeatedly circulate inside the microresonator. The WGM microlaser provides a highly limited light

field through the total internal reflection of optical microcavity and standing wave formation. The gain dye compensates for the loss and enhances the light field intensity by absorbing the pump light and providing stimulated emission. The combination of the two makes the microsphere structure realize stable whispering gallery mode laser under resonant condition[29]. When the target molecules combined with the aptamer, a G-quadruplex structure was formed, causing fluctuations in the RI of LC molecules at the LC/aqueous interface. Correspondingly, it would cause the WGM laser spectral shifts. If the spectral shift was resolved, it could be used as a readout for biomolecular detection.

As shown in Fig. 1, by functionalizing the surface of the WGM resonator, highly specific binding to biomolecules could be achieved. To form the microlaser probe, the microcavity was functionalized with two recognition elements: CTAB and DNA aptamer. The DNA aptamer can specifically recognize and bind NOX with a high affinity. Therefore, the target molecule can be selectively immobilized on the surface of the microresonator, resulting in changes in the RI at the microsphere interface. Upon irradiation with a 532 nm pulsed laser, the microlaser emitted laser signals. In comparison with the original laser spectrum, a wavelength shift occurred after NOX binding. The concentration of NOX was quantified by measuring the wavelength shift in the WGM lasing spectrum.

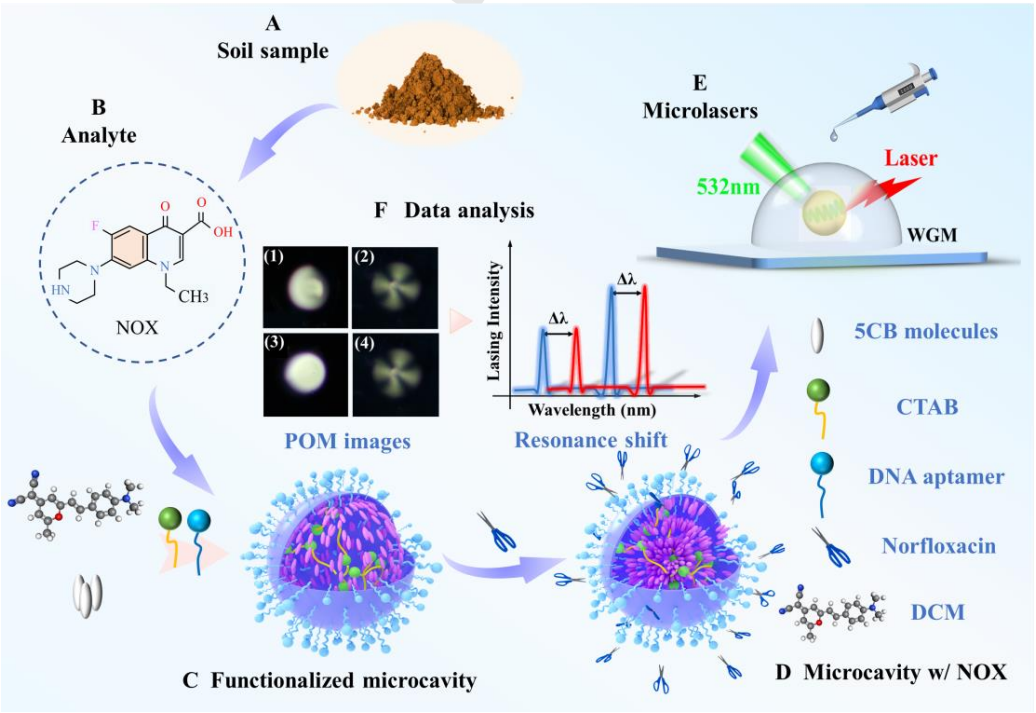

Fig. 1 Working Principle of Norfloxacin specific recognition based on LC microlaser.

3 Results and Discussions

Microlaser Emission. The optical system for laser emission of active mode LC microdroplets was shown in Fig. 2(a). Considering the use of a 532 nm pump light source and the need for good solubility and stability of dyes in LC materials, DCM(4-

(dicyanomethylene)-2-methyl-6-(4-dimethylaminostyryl)-4H-pyran) was chosen as a gain dye. The pump light energy was focused on the LC microdroplet via the microscope. A droplet of PBS droplet placed on a PMMA substrate functioned as the main medium for forming the LC microlasers. Since the refractive index of the microdroplet was higher than that of the external solution, the WGM laser was generated by appropriate excitation. The light emitted by the LC microdroplets was coupled to the optical fiber spectrometer through the microscope system. The reason for choosing DCM-LC was 3-fold: (1) LC microdroplets possessed nearly perfect spherical geometry and a smooth surface. It had a sufficient refractive index contrast with the test medium (H_2O), which was conducive to total internal reflection. (2) Side coupling with the micro-resonator could be avoided. The laser properties can be solved by free space optics. (3) Easy to fabricate. Under optimal excitation conditions, standard WGM laser emissions could be detected. The size uniformity of the prepared LC microdroplets is excellent.

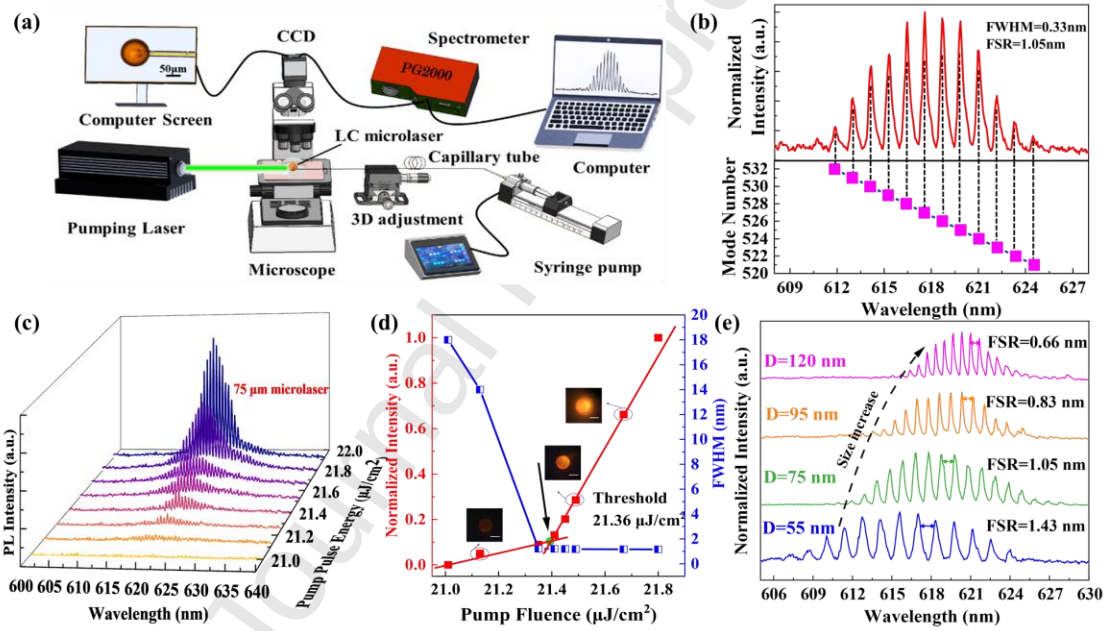

Fig.2 (a) Schematic Diagram of Working Principle. (b) WGM lasing observed in 75 μm microlaser. (c) Power dependent emission spectra of the 75 μm microlaser. (d) Dependence of normalized PL intensity and FWHM on pump fluence. The lasing threshold was determined at 21.36 μJ/cm². (e) WGM lasing with different microlasers diameters in PBS solution.

To characterize the laser behavior, a series of experiments were analyzed and verified the characteristics of WGM lasing in DCM-LC microdroplets from the lasing threshold, mode number and Q factor. The DCM-LC microdroplet was excited by a pulsed laser, generating the laser spectra as presented in Fig. 2(b). The sharp peaks detected in the spectrum verified the WGM lasing, and the measured laser spectrum was consistent with the first-order TE mode from 522 to 532[30]. The lasing threshold of microlaser was determined by collecting emission spectra at different pump pulse energies. Notably, a threshold PPE value of approximately 21.36 μJ/cm² was recorded, as depicted in Fig. 2(c). Fig. 2(d) illustrated the relationship between PL intensity and

FWHM of the emission peaks with respect to PPE. When the PPE exceeded the excitation threshold, a light ring appeared surrounding the DCM-5CB microlasers, and the emission brightness increased with higher excitation energy. The clear threshold behavior verified the lasing action from the microlasers.

Free spectral range (FSR) and quality factor Q were the other two important parameters of WGM. The FSR of LC microdroplets could be expressed as: $FSR=\lambda^2/2\pi nR$. n was the effective RI of the cavity medium, and R was the radius of the cavity. Fig. 2(e) showed the WGM laser spectra of LC microdroplets with different sizes. As the diameter of microdroplet increased from 55 μm to 120 μm, the FSR decreased from 1.43 nm to 0.66 nm. There was a linear correlation observed between FSR and 1/D. The quality factor Q represented the propagation loss of light in the cavity：$Q=\lambda/\Delta\lambda$[31]. The higher the Q, the smaller the loss of light in the cavity, which means that the resonance of the mode is stronger and the spectrum is narrower. The Q-factor for the WGM peaks reached approximately 2800, reflecting a strong resonance and narrow spectral width. To protect the dye quenching and the laser from the influence of overvoltage, 75 μm LC microdroplet was selected to achieve norfloxacin detection.

NOX-DNA aptamer Specific sensing. The microresonator was initially treated to enable high-precision target recognition during the sensing process. Therefore, the optimal concentration of CTAB and DNA aptamer were identified and illustrated, as shown in Fig.3[32]. Previous studies have indicated that LC microdroplets exhibiting parallel anchoring were defined as having bipolar configurations, while those with vertical anchoring correspond to radial configurations. 5CB microdroplets exhibited a bipolar configuration in pure DI or PBS solutions. However, the presence of different surfactants such as dodecyltrimethy-lammonium bromide (DTAB), sodium dodecyl sulfate (SDS), and CTAB at the LC/aqueous interface modified the anchoring energy at the surface. This alteration triggered a transition in the orientation state of the 5CB molecules, as shown in Fig. 3(a)(1).

With the increase of CTAB concentration, 5CB molecule transformed into radial configuration. Due to lateral hydrophobic interactions that CTAB and LC have undergone in their hydrocarbon regions, these interactions enable CTAB to self-assemble at the LC/ water interface[33]. When CTAB concentration was 1 μM, the structural transformation was completed. After that, the DNA aptamer was injected into the solution to observe the CTAB-aptamer complex formation. When the negatively charged aptamer was introduced, CTAB self-assembly at the interface was disrupted. The orientation of LC molecules was rearranged because of the electrostatic interaction between CTAB and DNA aptamer (Fig.3(a)(2)-(3)) [34]. The final configuration of LC microdroplets depended on the amount of DNA aptamers mixed, as shown in Fig.3(a)(4). When CTAB concentration was 1 μM and DNA aptamer concentration increased from 1 nM to 100 nM, significant changes in the configuration of 5CB microdroplets were observed. The radial structure essentially disappeared and

transformed into bipolar structure. However, when the DNA aptamer concentration exceeded 100 nM and no morphological changes were observed. The limited DNA aptamer concentration was determined to be 100 nM. When NOX was introduced, the aptamer, which originally had a coil-like structure, transformed into G-quadruplex structure. This structural shift restored the ability of CTAB to self-assemble at the LC/ aqueous interface. As a result, the system reverted to its initial homeotropic alignment, as shown in Fig.3(a) (5)–(8). Meanwhile, to verify the specific binding of aptamers, the non-aptamer sequence of the same length was selected as controls. The experimental results are shown in Fig.S1.

POM pattern could directly observe the morphology and configuration of liquid crystal droplets, and could be used as an indicator to test the concentration of norfloxacin, but this method still had some limitations. First of all, the morphological transformation of LC droplets was usually unpredictable and unstable, and it was difficult to identify the key characteristics in the polar transformation process of LC. Second, POM images could only provide qualitative information, and small optical changes could not be obtained. At the same time, subtle changes in the structure of liquid crystal droplets were difficult to distinguish in POM images. Therefore, WGM technology was used in LC microlaser detection of norfloxacin to improve the sensitivity and accuracy of detection.

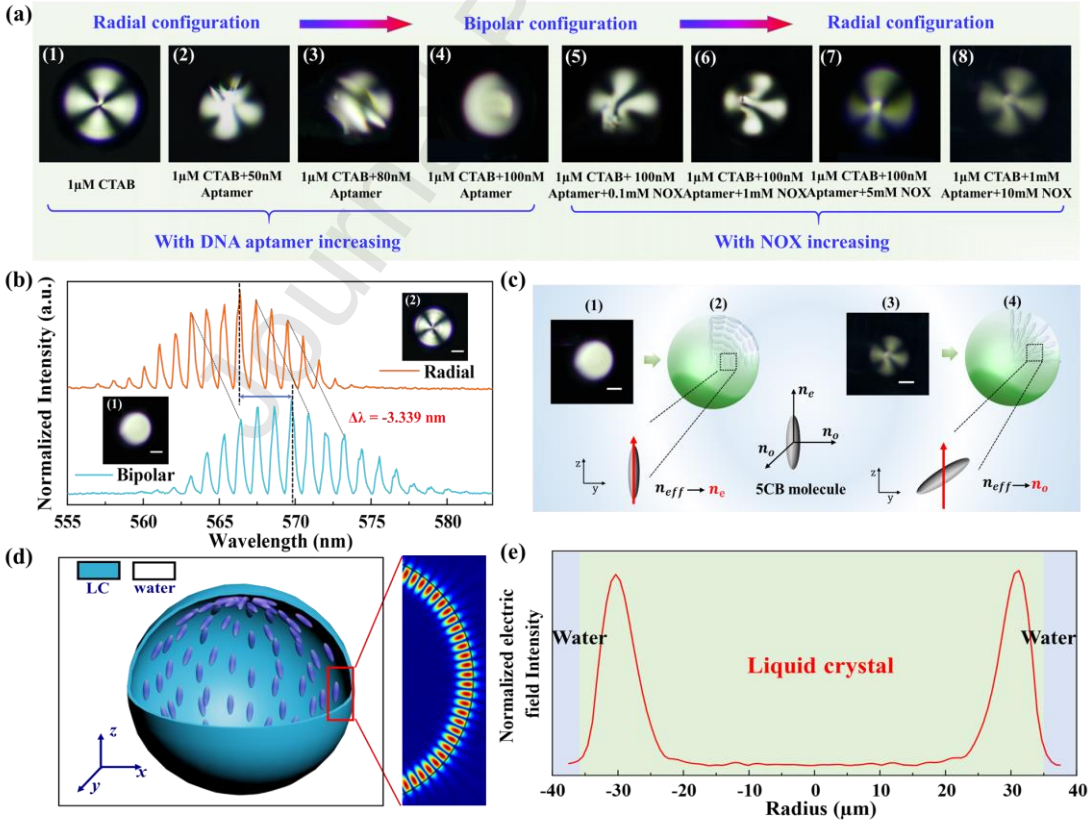

Fig.3 (a) POM images of the LC microdroplet during the structure transition. The scale was 50 μm. (b) WGM lasing of LC microlaser with the bipolar configuration and radial configuration. The insets show their POM images. (c) The transformation of 5CB molecules for different

configurations. (d) The Electric field distribution in the x-y plane of the microlaser. (e) Radially normalized field intensity distribution along the x-z plane.

In addition, the WGM spectral responses at different concentrations of norfloxacin were investigated, as shown in Fig. 3(b). When no concentration of norfloxacin was added, the functionalized liquid crystal microlaser presented a bipolar configuration, with the corresponding WGM spectral curve (blue curve). When 0.3 μg/mL of norfloxacin solution was added, the liquid crystal microdroplet presented a radial configuration and showed a significant blue shift trend in the corresponding WGM spectral curve (yellow curve). Due to the change in the concentration of the surrounding solution of the functionalized liquid crystal microdroplets, the resonance spectrum of the WGM laser shifted, verifying its potential as a sensor for detecting norfloxacin concentration.

The sensing of the WGM resonator was mainly based on the shift of the resonant wavelength of the resonator mode caused by the change of the surrounding environment of the microcavity. The LC microlaser was a bipolar configuration in the mixed solution of CTAB-DNA aptamer. The TE mode exhibited a large dielectric constant along the main axis of the 5CB molecules, which indicated a high refractive index n_e. After NOX was introduced, the 5CB molecules reoriented (Parallel - vertical). This rearrangement led to a gradual decrease in dielectric constant($n_o \leq n \leq n_e$), as shown in Fig. 3(c). The geometric structure of the LC microlaser was simulated using Ansys Lumerical FDTD and the electric field distribution within the microlaser was derived from numerical modeling. Based on experimentally measured parameters, the diameter of the LC microlaser (n_e=1.71, n_o=1.54) was defined as 75 μm. Simulation results showed that the electric field was predominantly localized near the periphery of the LC microdroplet, as depicted in Fig. 3(d). The intensity distribution of the mode field in Fig. 3(e) demonstrated that most of the energy remained contained within the microcavity.

DCM-5CB microdroplet had been functionalized by CTAB and NOX aptamer with concentrations of 1 μM and 100 nM, respectively. Then, a drop of the mixed solution of CTAB-DNA aptamer was placed onto the PMMA substrate, serving as the medium for microlaser. Before any binding events, only red green lasing peaks could be generated[35]. After adding an equal volume of NOX solution, the WGM spectrum exhibited a significant blue shift, as shown in Fig.4(a)-(b). All the experiments should be repeated at least three times. In the experiment the sensitivity of NOX detection was 13.2 nm/μg/mL, and the linear correlation value (R^2) was 0.983. The WGM resonance spectrum showed an obvious blue shift in the concentration range of 0-3×10^3 μg/mL. Fig. 4(c) depicted the spectral response time of WGM at different NOX concentrations, with the bar marks indicating the intervals of completed reactions. Specially, as the concentration of norfloxacin increased, the continuous blue shift of the WGM resonance peak occurs, with the wavelength steadily increasing from 0 to 330 s, then stabilizing at 330 to 360 s. This indicated that the reaction was completed within the

330-360 s, as shown in Fig. 4(c)(2). To verify that the WGM wavelength shift was caused by the addition of norfloxacin, the WGM spectrum generated from the initial CTAB-DNA aptamer solution served as a control experiment. During 300 s observation period, no significant shift was detected. Therefore, changes in the resonant wavelength of LC microcavities were considered to the perturbation of interest to us.

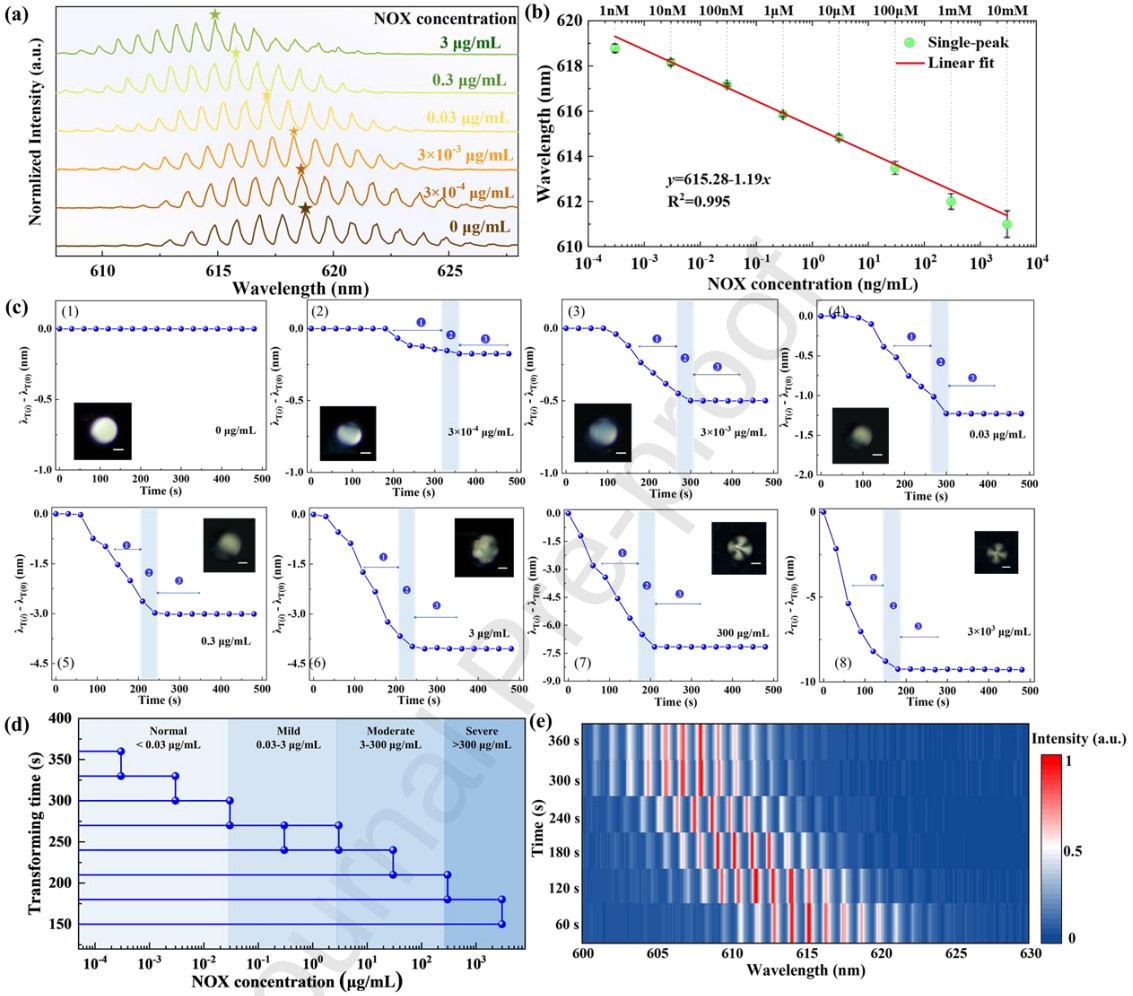

Fig.4 (a) WGM spectral of functionalized 5CB microlasers under various NOX concentrations. As NOX concentration increased, the spectrum was blue shifted. (b) Fitting curve of NOX concentration detection sensitivity. All experiments were repeated three times. (c) Spectral responses for different NOX concentrations: (1) 0 μg/mL; (2) 3×10^{-4} μg/mL; (3) 3×10^{-3} μg/mL; (4) 0.03 μg/mL; (5) 0.3 μg/mL; (6) 3 μg/mL; (7) 300 μg/mL; (8) 3×10^{4} μg/mL. The inset showed the POM images of DCM-LC microdroplets at different concentrations. The scale was 50 μm. (e) Transforming time for different NOX concentrations. (d) The WGM spectrum of 0.3×10^{3} μg/mL NOX, recorded every 60 s.

Fig. 4(d) presented an analysis of the wavelength shifts occurring at adjacent time intervals within each completed reaction cycle. Notably, the spectral migration rate was stable under different concentrations, as could be proved by the consistent shift of WGM spectral wavelength migration over time in the response time curve. By correlating these spectral shifts with the reaction time, the concentration of norfloxacin can be quickly classified as normal

(<0.03 μg/mL), mild (0.03-3 μg/mL), moderate (3-300 μg/mL) or severe (>300 μg/mL) environmental hazards, thereby facilitating an effective assessment of the severity of environmental pollution. Although POM images remained almost unchanged in the 0.3×10^3 μg/mL and 3×10^3 μg/mL concentration, the WGM spectrum observed an obvious shift. The results further validated the enhancement capability of WGM technique in identifying minor alterations in eigenmodes. For ongoing monitoring, the WGM spectrum of 0.3×10^3 μg/mL NOX concentration was tracked, as shown in Fig.4(e). Meanwhile, this behavior also demonstrates that LC-WGM sensor can analyze and record the resonance spectral characteristics of different concentrations of norfloxacin solutions has high reproducibility and long-term stability.

The specificity and selectivity of NOX sensor. To evaluate the selectivity and specificity of this biosensor, six different drugs were chosen: amoxicillin (AMX), tetracycline (TCY), paracetamol (PCM), ciprofloxacin (CPR), Enrofloxacin (ENR) and levofloxacin (LEV). AMX and TCY were an antibiotic drug similar to NOX, while PCM, which treated minor infections, was not classified as an antibiotic. The remaining compounds were part of the fluoroquinolone (FQ) family[36].

To verify the specificity of the sensor, the experiment was specifically conducted using the control group and the model group, as shown in Fig. 5(a). AMX (50 nM, 20.9 ng/mL), TCY (50 nM, 22.2 ng/mL), PCM (50 nM, 7.6 ng/mL), NOX (50 nM, 15.9 ng/mL) were incubated together with the CTAB-DNA aptamer solution mixture, respectively. Fig.S2 showed the POM images of DCM-LC microdroplet and the mixture of different drug-CTAB-DNA aptamers. It could be found that LC microdroplet in the solutions presented bipolar configuration. The spectra deviation of WGM spectrum under several drugs were also studied. Notably, only NOX caused a significant blue wavelength shift compared to three prescription drugs, as presented in Fig.S3. This result emphasized that NOX engaged in a targeted interaction with the DNA aptamer, reactivating the LC-CTAB interface response. This reactivation was associated with a shift in the LC's RI and the appearance of a shortened wavelength.

To investigate the selectivity of biosensors in fluoroquinolone (FQ) family members, DCM-5CB was placed in the CPR (5 nM, 1.7 ng/mL)-DNA aptamer, ENR (5 nM, 1.8 ng/mL)-DNA aptamer, LEV (5 nM, 1.8 ng/mL)-DNA aptamer and NOX (5 nM, 1.59 ng/mL)-DNA aptamer solution, respectively. Spectral shift was observed only in NOX-DNA aptamer solution. These findings indicated that the DNA aptamer probe exhibited strong binding affinity for NOX, even in the presence of other FQ family, as demonstrated in Fig. S3 and Fig.5(b). All the experiments were repeated at least three times. The experimental results show that the sensor has good repeatability.

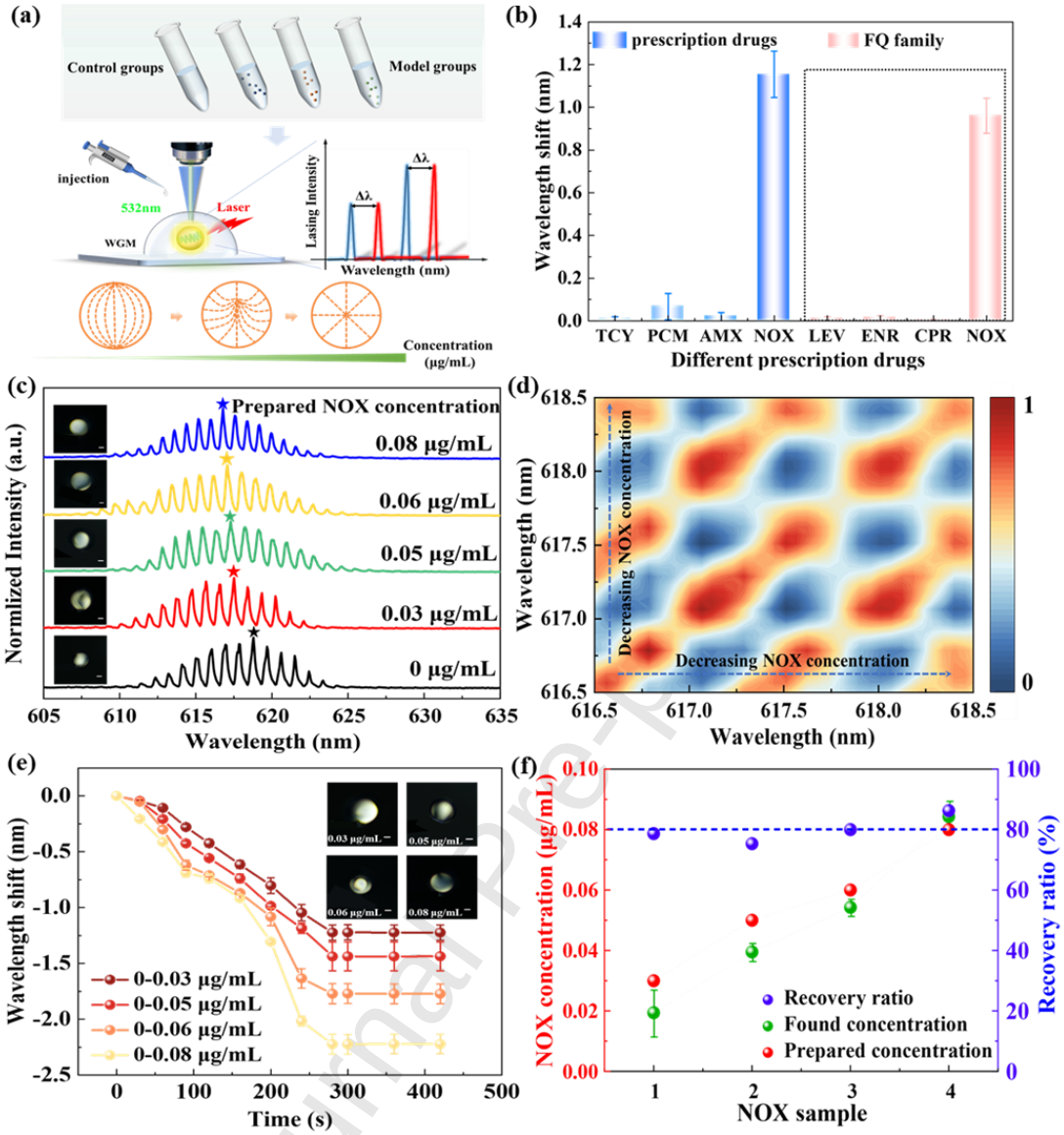

Fig. 5 (a) Schematic illustration of NOX detection specificity analysis. (b) The wavelength shift of eight different drugs. (c) WGM spectral response of soil samples with different NOX concentrations. (d) 2D correlation spectra of the same mode for decreasing NOX concentration. (e) Response time curve of NOX concentration in different soil samples. (f) Recovery of NOX sensing in soil samples. All the experiments were repeated at least three times.

Real sample detection. As an environmental micro-pollutant, Norfloxacin had attracted wide attention due to its widespread presence in environmental media such as water bodies and soil, and its potential risks to human health. When the content of norfloxacin in the soil exceeds 0.1 μg/mL(300nM), it will affect the inhibition of plant growth, the activity of enzymes, and pose a significant risk to the agricultural ecosystem. To monitor NOX usage and detect its presence in the soil, samples were collected from a certain area of the Lingshui Lake. Four different concentrations of soil sample solutions were prepared, respectively: 0.03 μg/mL(100nM), 0.05 μg/mL(150nM), 0.06 μg/mL(200nM), 0.08 μg/mL(250nM). 75 μm of microlasers in a soil sample containing 0.08 μg/mL NOX, the wavelength shift of the laser spectrum within 10 mins

was about 2.2 nm, as shown in Fig.5(c) and Fig.S4. Fig.5(d) showed the WGM resonance spectra of the same transmission mode shifted to shorter wavelengths because of the increase in norfloxacin concentration. The response time and wavelength deviation of the laser probe in NOX soil samples were also proved through experiments, as shown in Fig.5(e) and Fig.S5. It was observed that the response speed of NOX exhibited a positive correlation with the reaction time. The higher the concentration of NOX, the faster the response time and the larger the wavelength shift. The response time was basically stable at 300 s. Fig.5(f) showed a summary of the NOX detection results in soil samples, along with relative deviations, demonstrating high consistency and reliability with recovery rates ranging from 75.3% to 86.3%. Meanwhile, to evaluate the accuracy of this analytical method, the HPLC method was used to measure the spiked samples, as shown in Table 1. The established spectra analysis results are in good agreement with the HPLC analysis method, indicating that this method can be used for the detection of norfloxacin in soil. Although it has met the methodological requirements of most environmental analyses of 70% - 120%[37], there is still a gap compared to the theoretical 100%. The reasons for the recovery rate of norfloxacin are mainly closely related to various factors such as the strong adsorption effect of the soil, the matrix effect, and the limitations of extraction conditions[38–40].

Table1 Liquid crystal biosensor detects NOX in soil (n=3).

Added (μg/mL)	WGM lasing based LC sensor		HPLC	
	Recovery (%)	RSD (%)	Recovery (%)	RSD (%)
0.03	78.6	0.55	80.02	0.71
0.05	75.3	0.21	76.06	1.05
0.06	80	0.2	82.13	0.86
0.08	86.25	0.36	85.14	2.26

The detection capability of the prepared biosensor was evaluated against other methods for NOX concentration detection, with the results summarized in Table 2. In general, a variety of methods for detecting norfloxacin have been developed, including electrochemical sensing[41], high performance liquid chromatography (HPLC)[42], fluorescence spectrophotometry[43], and dark-light optical imaging[44], respectively. Each method has its own advantages and disadvantages. Compared with the detection method based on POM, the biosensor constructed in this study can achieve real-time quantitative monitoring of the reaction process, be capable of distinguishing minute signal changes, and have the ability to detect analytes at low concentrations. Although the methods based on fluorescence intensity ratio or oxidation peak current in the literature show similar performance in terms of detection limit, they often come with problems such as unstable selectivity, significant background interference, or complex operation. Similarly, other detection methods using the same aptamer[43,44], although having comparable detection limits, often encounter limitations such as fluorescence quenching or cumbersome probe synthesis procedures. In this experiment, the

maximum sensitivity of Norfloxacin Detection was 13.2 nm/μg/mL. The detection limit of norfloxacin measured was 0.3 ng/mL. The detection limit has been increased by one order of magnitude compared with the traditional POM method. Notably, at detected 0.3×10^3 μg/mL and 3×10^3 μg/mL NOX concentrations, LC microdroplets exhibited the same radial configuration but distinct spectral shift behaviours. This highlighted that leveraging the WGM spectral response for detecting the reaction process offered greater accuracy than relying on simple POM observation. The enhancement of light-matter interaction within the microcavity has elevated the capability for detecting faint signals, thereby facilitating enhanced sensitivity, detection limits, and monitoring ranges for NOX sensing.

Table 2 Compares different types of biosensors for NOX detection.

Sensor structure	Detection method	Detection range	Detection limit	Ref.
molecularly imprinted silica polymers	HPLC	0.01-1 μg/mL	1.92 ng/mL	[42]
Carbon dots/metal organic framework composite	fluorescence detection	0.3-2.6 μg/mL	26.2 ng/mL	[45]
g-C_3N_4/MOFs photoresponsive oxidase mimic	photoelectrochemical	0.003-0.64 μg/mL	1.8 ng/mL	[46]
molecularly imprinted polymers modified Electrode	electrochemical	0.03-51.1 μg/mL	1.3 ng/mL	[47]
LC at aqueous interface	Dark-bright optical image	3×10^{-4}-0.03μg/mL	1.6 ng/mL	[44]
Tb^{3+}ion-NOX aptamer probe	Spectrofluorometry	0.001–0.1 μg/mL	0.02 ng/mL	[43]
WGM lasing based LC sensor	WGM resonance spectra	3×10^{-4}-3×10^3 μg/mL	0.3 ng/mL	This work

Conclusions

In this study, a highly sensitive biosensor for detecting norfloxacin was developed, utilizing a DNA aptamer as the target recognition probe in conjunction with a LC-based biosensing strategy. The binding of the DNA aptamer to norfloxacin induced CTAB to redistribute at the LC/water interface, which led to the realignment of LC molecules in the vertical direction. When combined with whispering gallery mode (WGM) spectroscopy, this change enabled the detection of norfloxacin at concentrations as low as 0.3 ng/mL. This proposed sensing approach was characterized by its simplicity, convenience, label-free operation, and high sensitivity. In addition, the biosensor demonstrated strong selectivity for norfloxacin over other antibiotics and related compounds. These properties make it an attractive method for highly specific detection of lake water, soil samples and other potential applications.

Experimental section/methods

Materials and chemicals

For microcavity modification, nematic liquid crystal 4-cyano-4′-pentylbiphenyl (5CB), hexadecyl trimethyl ammonium bromide (CTAB), phosphate-buffered saline (PBS, pH=7.4) were purchased from Aladdin. The DNA aptamer specific sequence 5′-CCC ATC AGG GGG CTA GGC TAA CAC GGT TCG GCT CTC TGA GCC CGG GTT ATT TCA GGG GGA-3′ was synthesized by synbio Technologies. The DNA aptamer was selected from previously reported[32]. For specific recognition experiment, norfloxacin (NOX, ≥98%); amoxicillin trihydrate (AMX, ≥98%), tetracycline (TCY, ≥98%), paracetamol (PCM, ≥98%); ciprofloxacin (CPR, 99.9%), enrofloxacin (ENR, 99.9%), levofloxacin (LVO, 99.9%) were purchased from Aladdin. 4-dicyano-methylene-2-methyl-6-(4-dimethylaminostyryl) −4H-pyan (DCM) serving as the gain media, was purchased from Bidepharm. All aqueous solutions were prepared using deionized (DI) water from the Milli-Q system (Millipore, USA) at room temperature.

Preparation of the solution to be tested

The test sample was prepared with PBS solution in the experiment. CTAB and norfloxacin (NOX) solutions at different concentrations were obtained by dissolving measured weighed amounts. The NOX aptamer stock was diluted at room temperature for further experiments. During the experiment, the optimal concentrations for CTAB and DNA aptamer, corresponding to a microdroplet configuration of bipolar-radial-bipolar, were first observed to be 1 μM and 100 nM, respectively. The CTAB and NOX aptamer complex was produced by mixing the two working solutions in equal volumes and incubating at 37°C for at least 30 mins. For NOX concentration detection, equal volume of NOX sample and 100 nM aptamer were combined and kept for 1.5 h, and then the same volume of 1 μM CTAB solution was added. The same LC microdroplet can be used to achieve continuous measurement of different norfloxacin concentrations. Each assay was repeated many times to confirm reproducibility.

Preparation of 5CB microlasers

The 5CB microdroplets (n_e=1.71, n_o=1.54) doped with DCM served as the fundamental component of the sensor probe. Depending on the self-assembly properties of LC molecules, 5CB microdroplets were readily generated from self-made capillary tubes, with an inner core diameter of approximately 4 μm. In order to generate WGM laser, it was necessary to participate in DCM dyes. The DCM concentration was 0.1 wt%. First, DCM was added to 5CB. Then, the mixture underwent ultrasonic treatment for 30 minutes to achieve thorough dissolution and homogeneity. Following sonication, the DCM-doped 5CB sample was transferred to a small reagent vial for later use. The size of the 5CB microdroplets was regulated by adjusting the syringe pump injection speed in the liquid medium.

Preparation and Analysis of real samples

To assess the practical applicability of the sensor probe, real soil samples were collected from a certain area of Lingshui Lake for NOX determination. To analyze the

soil samples, 10 g soil was added to 100 mL 1 μg/mL (3μM) NOX solution prepared in DI water. The mixture was stirred at room temperature for 1 h to ensure thorough interaction. Subsequently, the mixture was filtered using filter paper, and the filtrate was collected as a stock solution containing 1 μg/mL (300nM) of NOX. This stock solution was continuously diluted with DI water to obtain NOX concentrations of 0.03 μg/mL (100nM), 0.05 μg/mL(150nM), 0.06 μg/mL(200nM), 0.08 μg/mL (250nM) for further analysis. Norfloxacin was determined by high performance liquid chromatography *(HPLC, Vanquish C, Thermo)*. A C18 reversed-phase column (4.6×250 mm, 5 μm, *Thermo Scientific™ Acclaim™*) enabled chromatographic separation. The mobile phase was 40% Methanol and 60% phosphate buffer. UV absorption wavelength was 278 nm. The flow rate was 1.0 mL/min and the injection volume was 5 μL. The initial samples were tested and norfloxacin was not detected. Norfloxacin was determined by two methods to assess the practicality and accuracy of the sensor.

Optical measurement

Firstly, by adjusting the syringe pump speed and injection time, the radius of 5CB microdroplets were prepared in the measured solution. The microscopic system (SOPOP, BH200M) was employed for exciting the active WGM system and collecting laser spectroscopy. Optical pumping was performed using the Nd:YAG pulsed laser (Ltd DPS-532-A, Changchun New Industries Optoelectronics Tech. Co., China). The pulsed light was irradiated onto the DCM-5CB microlaser by the microscopic system. To prevent degradation of dye molecules, the microdroplets were excited briefly (about 1 s) for spectral recording. The WGM spectrum was fed into the spectrometer (PG2000, Ideaoptics Technology Ltd., China) by the coupler to be recorded. The image was observed using a polarized optical microscope (POM, BX41P，Olympus，Japan). Each experimental group was repeated at least three times to minimize the impact of environmental interference.

Author contributions

Peiyao An: conceptualization, investigation, methodology, and writing original draft. **Mengxiao Li:** investigation, methodology. **Shanshan Zhang:** analyse the experimental results. **Zhenqi Cao:** writing review, editing. **Miao Yu:** investigation. **Tang cheng Huang:** methodology. **Duo Wang:** methodology. **Yue Li:** investigation. **Rensheng Shen:** supervision. **Xin Yang:** supervision. **Jun Ren:** supervision and project administration. **Zhenlin Wu:** supervision and project administration. All authors contributed to the general discussion.

Conflicts of interest

There are no conflicts to declare.

Acknowledgements

This work was funded by project "Fundamental Research Funds for the Central Universities (DUT25YG256)".

Reference

[1] M. Li, L. Luo, J. Li, Y. Xiong, L. Wang, X. Liu, Colorimetric Chemosensor Based on Fe_3O_4 Magnetic Molecularly Imprinted Nanoparticles for Highly Selective and Sensitive Detection of Norfloxacin in Milk, Foods 12 (2023) 285.

[2] S. Sivaselvam, R.S. Anjana, N.S. Dhujana, M. Victor, R.S. Jayasree, Nitrogen-doped carbon dots: a novel biosensing platform for selective norfloxacin detection and bioimaging, J. Mater. Chem. B 12 (2024) 7635–7645.

[3] Z. Wang, B. Song, J. Li, X. Teng, Degradation of norfloxacin wastewater using kaolin/steel slag particle electrodes: Performance, mechanism and pathway, Chemosphere 270 (2021) 128652.

[4] Z. Chi, Q. Wang, J. Gu, Recent advances in colorimetric sensors based on nanozymes with peroxidase-like activity, Analyst 148 (2023) 487–506.

[5] W. Lu, Y. Jiao, Y. Gao, J. Qiao, M. Mozneb, S. Shuang, C. Dong, C. Li, Bright Yellow Fluorescent Carbon Dots as a Multifunctional Sensing Platform for the Label-Free Detection of Fluoroquinolones and Histidine, ACS Appl. Mater. Interfaces 10 (2018) 42915–42924.

[6] S. Lu, Y. Zhang, J. Liu, C. Zhao, W. Liu, R. Xi, Preparation of anti-Pefloxacin Antibody and Development of an Indirect Competitive Enzyme-Linked Immunosorbent Assay for Detection of Pefloxacin Residue in Chicken Liver, J. Agric. Food Chem. 54 (2006) 6995–7000.

[7] X. Liu, Z. Xu, Z. Han, L. Fan, S. Liu, H. Yang, Z. Chen, T. Sun, B. Ning, A highly sensitive and dual-readout immunoassay for norfloxacin in milk based on QDs-FM@ALP-SA and click chemistry, Talanta 234 (2021) 122703.

[8] L. Chierentin, H.R.N. Salgado, Review of Properties and Analytical Methods for the Determination of Norfloxacin, Critical Reviews in Analytical Chemistry 46 (2016) 22–39.

[9] V.F. Samanidou, C.E. Demetriou, I.N. Papadoyannis, Direct determination of four fluoroquinolones, enoxacin, norfloxacin, ofloxacin, and ciprofloxacin, in pharmaceuticals and blood serum by HPLC, Anal Bioanal Chem 375 (2003) 623–629.

[10] Z. Wang, J. Li, X. Liu, J. Yang, X. Lu, Preparation of an amperometric sensor for norfloxacin based on molecularly imprinted grafting photopolymerization, Anal Bioanal Chem 405 (2013) 2525–2533.

[11] N. Yang, Q.-L. Wen, Y.-B. Fu, L.-F. Long, Y.-J. Liao, S.-B. Hou, P. Qian, P. Liu, J. Ling, Q. Cao, A lead-free Cs2ZnCl4 perovskite nanocrystals fluorescent probe for highly selective detection of norfloxacin, Spectrochimica Acta Part A: Molecular and Biomolecular Spectroscopy 281 (2022) 121568.

[12] M. Sadati, A.I. Apik, J.C. Armas-Perez, J. Martinez-Gonzalez, J.P. Hernandez-Ortiz, N.L. Abbott, J.J. De Pablo, Liquid Crystal Enabled Early Stage Detection of Beta Amyloid Formation on Lipid Monolayers, Adv Funct Materials 25 (2015) 6050–6060.

[13] T.T. Phan, J.H. Harwell, D.A. Sabatini, Effects of Triglyceride Molecular Structure on Optimum Formulation of Surfactant-Oil-Water Systems, J Surfact & Detergents 13 (2010) 189–194.

[14] J.M. Brake, M.K. Daschner, Y.-Y. Luk, N.L. Abbott, Biomolecular Interactions at

Phospholipid-Decorated Surfaces of Liquid Crystals, Science 302 (2003) 2094–2097.

[15] V.K. Gupta, J.J. Skaife, T.B. Dubrovsky, N.L. Abbott, Optical Amplification of Ligand-Receptor Binding Using Liquid Crystals, Science 279 (1998) 2077–2080.

[16] C.-H. Chen, K.-L. Yang, A liquid crystal biosensor for detecting organophosphates through the localized pH changes induced by their hydrolytic products, Sensors and Actuators B: Chemical 181 (2013) 368–374.

[17] P. An, X. Hao, S. Zhang, M. Li, C. Wang, M. Yang, M. Yu, J. Ren, R. Shen, Z. Wu, Ultra-sensitive liquid crystal-coated microbubble resonator based on a whispering gallery mode for penicillin G detection, Opt. Lett. 49 (2024) 7230.

[18] X. Hao, M. Li, S. Zhang, M. Yu, P. An, C. Wang, M. Yang, J. Ren, R. Shen, Z. Wu, Quantitative monitoring of enzymatic reactions using pH optical barcodes from high Q-factor microbubble resonators, Optics & Laser Technology 183 (2025) 112188.

[19] X. Ding, K.-L. Yang, Liquid crystal based optical sensor for detection of vaporous butylamine in air, Sensors and Actuators B: Chemical 173 (2012) 607–613.

[20] Z. Wang, Y. Liu, C. Gong, Z. Yuan, L. Shen, P. Chang, K. Liu, T. Xu, J. Jiang, Y.-C. Chen, T. Liu, Liquid crystal-amplified optofluidic biosensor for ultra-highly sensitive and stable protein assay, PhotoniX 2 (2021) 18.

[21] J. Liao, L. Yang, Optical whispering-gallery mode barcodes for high-precision and wide-range temperature measurements, Light Sci Appl 10 (2021) 32.

[22] H. Yu, O. Alkhamis, J. Canoura, Y. Liu, Y. Xiao, Advances and challenges in small-molecule DNA aptamer isolation, characterization, and sensor development, Angew. Chem. Int. Ed. 60 (2021) 16800–16823.

[23] S. Stangherlin, N. Lui, J.H. Lee, J. Liu, Aptamer-based biosensors: From SELEX to biomedical diagnostics, TrAC Trends in Analytical Chemistry 191 (2025) 118349.

[24] M. He, Z. Wang, X. Wu, Z. Du, C. Cui, Z. Zhao, Y. Sun, X. Zhang, L. He, W. Tan, Functional SELEX and biomedical applications of aptamers: beyond molecular recognition, Angew. Chem. Int. Ed. 64 (2025) e202424687.

[25] W. Bao, G. Aodeng, L. Ga, J. Ai, Nucleic acid aptamer-based biosensor for health monitoring: A review and future prospects, Microchemical Journal 214 (2025) 113894.

[26] A. Verdian, Z. Rouhbakhsh, E. Fooladi, An ultrasensitive platform for PCB77 detection: New strategy for liquid crystal-based aptasensor fabrication, J. Hazard. Mater. 402 (2021) 123531.

[27] H.J. Kim, C.-H. Jang, Liquid crystal-based aptasensor for the detection of interferon-γ and its application in the diagnosis of tuberculosis using human blood, Sensors and Actuators B: Chemical 282 (2019) 574–579.

[28] S. Mostajabodavati, M. Mousavizadegan, F.M. Moghadam, M. Mohammadimasoudi, M. Hosseini, Non-invasive cortisol monitoring via a machine leaning-enabled smartphone liquid crystal aptasensor, Microchem. J. 214 (2025) 113944.

[29] M. Suo, Y. Fu, S. Wang, S. Lin, J. Zhang, C. Wu, H. Yin, P. Wang, W. Zhang, X.-H. Wang, Miniaturized Laser Probe for Exosome-Based Cancer Liquid Biopsy, Anal. Chem. 96 (2024) 1965–1976.

[30] S. Yang, Y. Wang, H. Sun, Advances and Prospects for Whispering Gallery Mode Microcavities, Advanced Optical Materials 3 (2015) 1136–1162.

[31] R. Duan, Z. Zhang, L. Xiao, X. Zhao, Y.T. Thung, L. Ding, Z. Liu, J. Yang, V.D. Ta, H. Sun, Ultralow-Threshold and High-Quality Whispering-Gallery-Mode Lasing from Colloidal

Core/Hybrid-Shell Quantum Wells, Advanced Materials 34 (2022) 2108884.

[32] H. Ni, S. Zhang, X. Ding, T. Mi, Z. Wang, M. Liu, Determination of enrofloxacin in bovine milk by a novel single-stranded DNA aptamer chemiluminescent enzyme immunoassay, Anal. Lett. 47 (2014) 2844–2856.

[33] H. You, Z. Mu, M. Zhao, J. Zhou, Y. Chen, L. Bai, Voltammetric aptasensor for sulfadimethoxine using a nanohybrid composed of multifunctional fullerene, reduced graphene oxide and Pt@Au nanoparticles, and based on direct electron transfer to the active site of glucose oxidase, Microchim Acta 186 (2019) 1.

[34] P.S. Noonan, R.H. Roberts, D.K. Schwartz, Liquid Crystal Reorientation Induced by Aptamer Conformational Changes, J. Am. Chem. Soc. 135 (2013) 5183–5189.

[35] Z. Wang, G. Fang, Z. Gao, Y. Liao, C. Gong, M. Kim, G.-E. Chang, S. Feng, T. Xu, T. Liu, Y.-C. Chen, Autonomous Microlasers for Profiling Extracellular Vesicles from Cancer Spheroids, Nano Lett. 23 (2023) 2502–2510.

[36] H. Yi, Z. Yan, L. Wang, X. Zhou, R. Yan, D. Zhang, G. Shen, S. Zhou, Fluorometric determination for ofloxacin by using an aptamer and SYBR Green I, Microchim Acta 186 (2019) 668.

[37] M. Shen, Y. Hu, K. Zhao, C. Li, B. Liu, M. Li, C. Lyu, L. Sun, S. Zhong, Occurrence, bioaccumulation, metabolism and ecotoxicity of fluoroquinolones in the aquatic environment: A review, Toxics 11 (2023) 966–988.

[38] M. Sun, Y. Yang, M. Huang, S. Fu, Y. Hao, S. Hu, D. Lai, L. Zhao, Adsorption behaviors and mechanisms of antibiotic norfloxacin on degradable and nondegradable microplastics, Science of The Total Environment 807 (2022) 151042.

[39] W. Liao, V. Sharma, S. Xu, Q. Li, L. Wang, Microwave-enhanced photolysis of norfloxacin: Kinetics, matrix effects, and degradation pathways, IJERPH 14 (2017) 1564.

[40] N. Sun, H. Wang, X. Zhang, Z. Chen, A. Peng, Clay minerals-mediated removal of Norfloxacin and Norfloxin-resistant bacteria from water environments and associated mechanisms, Environ. Sci. Pollut. Res. 31 (2024) 67024–67034.

[41] S.M. Taghdisi Heidarian, A. Tavanaee Sani, N.M. Danesh, M. Ramezani, M. Alibolandi, G. Gerayelou, K. Abnous, S.M. Taghdisi, A novel electrochemical approach for the ultrasensitive detection of fluoroquinolones based on a double-labelled aptamer to surpass complementary strands of aptamer lying flat, Sens. Actuators, B 334 (2021) 129632.

[42] D. Qin, M. Zhao, J. Wang, Z. Lian, Selective extraction and detection of norfloxacin from marine sediment and seawater samples using molecularly imprinted silica sorbents coupled with HPLC, Mar. Pollut. Bull. 150 (2020) 110677.

[43] J. Chen, Y. Jin, T. Ren, S. Wang, X. Wang, F. Zhang, Y. Tang, A novel terbium (III) and aptamer-based probe for label-free detection of three fluoroquinolones in honey and water samples, Food Chemistry 386 (2022) 132751.

[44] S. Das, S. Sil, S.K. Pal, P. Kula, S. Sinha Roy, Label-free liquid crystal-based optical detection of norfloxacin using an aptamer recognition probe in soil and lake water, Analyst 149 (2024) 3828–3838.

[45] S. Wu, C. Chen, J. Chen, W. Li, M. Sun, J. Zhuang, J. Lin, Y. Liu, H. Xu, M. Zheng, X. Zhang, B. Lei, H. Zhang, Construction of carbon dots/metal–organic framework composite for ratiometric sensing of norfloxacin, J. Mater. Chem. C 10 (2022) 15508–15515.

[46] S. Yang, J. Chen, L. Yan, Y. Liu, W. Zha, Z. Fang, J. Zhang, Molecularly imprinted

photoelectrochemical sensing platform based on g-C3N4/MOFs photoresponsive oxidase mimic for norfloxacin detection, Microchem. J. 196 (2024) 109607.

[47] J. Yuan, H. Zhang, H. Shi, G. Zhang, S. Feng, Molecularly imprinted polymer modified electrode prepared by in situ polymerization for specific determination of norfloxacin, J. Electrochem. Soc. 169 (2022) 117509.

Declaration of interests

☒ The authors declare that they have no known competing financial interests or personal relationships that could have appeared to influence the work reported in this paper.

☐ The authors declare the following financial interests/personal relationships which may be considered as potential competing interests:

Graphical Abstract：

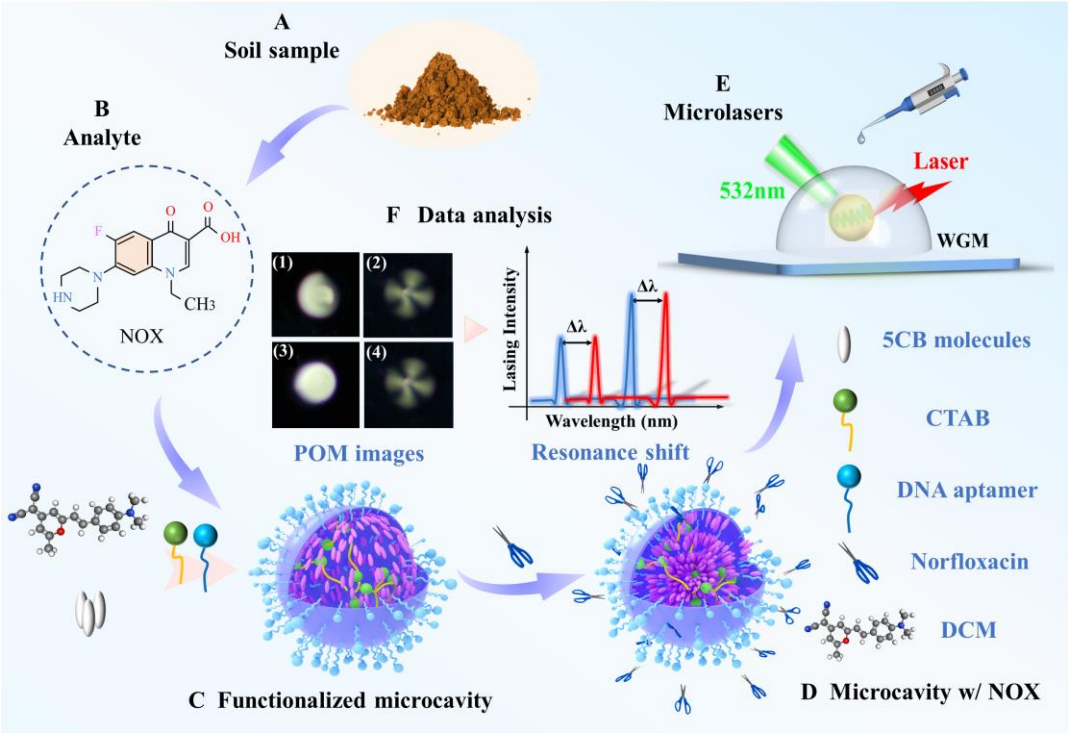

Fig.1 Working Principle of Norfloxacin specific recognition based on LC microlaser.

Highlights:

1. A aptamer-LC biosensor based on whispering gallery mode laser was proposed for NOX detection.
2. The limit of detection for NOX is as low as 0.3 ng/mL via dual amplification from LC and WGM resonance.
3. By monitoring the WGM spectra shift, real-time observation of the NOX reaction is achieved.
4. The biosensor provides an ideal sensing platform for complex biomedical samples detection.